Simulating rare kaon decays $K^+ \to \pi^+ \ell^+ \ell^-$ using domain wall lattice QCD with physical light quark masses

P. A. Boyle,[1,2] F. Erben,[1] J. M. Flynn,[3,4] V. Gülpers,[1] R. C. Hill,[1,3] R. Hodgson,[1] A. Jüttner,[3,4,5]
F. Ó hÓgáin,[1] A. Portelli,[1,*] and C. T. Sachrajda[3]

(RBC and UKQCD Collaborations)

[1]*School of Physics and Astronomy, University of Edinburgh, Edinburgh EH9 3JZ, United Kingdom*
[2]*Physics Department, Brookhaven National Laboratory, Upton, New York 11973, USA*
[3]*School of Physics and Astronomy, University of Southampton, Southampton SO17 1BJ, United Kingdom*
[4]*STAG Research Centre, University of Southampton, Southampton SO17 1BJ, United Kingdom*
[5]*CERN, Theoretical Physics Department, 1211 Geneva 23, Switzerland*

We report the first calculation using physical light-quark masses of the electromagnetic form factor $V(z)$ describing the long-distance contributions to the $K^+ \to \pi^+ \ell^+ \ell^-$ decay amplitude. The calculation is performed on a $2+1$ flavor domain wall fermion ensemble with inverse lattice spacing $a^{-1} = 1.730(4)$ GeV. We implement a Glashow-Iliopoulos-Maiani cancellation by extrapolating to the physical charm-quark mass from three below-charm masses. We obtain $V(z = 0.013(2)) = -0.87(4.44)$, achieving a bound for the value. The large statistical error arises from stochastically estimated quark loops.

I. INTRODUCTION

The $K^+ \to \pi^+ \ell^+ \ell^-$ ($\ell = e, \mu$) decays are flavor-changing neutral current processes that are heavily suppressed in the standard model (SM), and thus expected to be sensitive to new physics. Their branching ratios, taken from the latest PDG average [1], are $\mathrm{Br}[K^+ \to \pi^+ e^+ e^-] = 3.00(9) \times 10^{-7}$ and $\mathrm{Br}[K^+ \to \pi^+ \mu^+ \mu^-] = 9.4(6) \times 10^{-8}$. This process is dominated by a single virtual-photon exchange ($K \to \pi \gamma^*$), whose amplitude is predominantly described by long-distance, nonperturbative physics [2]. With tensions between the LHCb measurement [3] of and SM predictions for the ratio R_K contributing to increased interest in lepton-flavor universality (LFU) violation, important tests of LFU in the kaon sector could also be provided by $K^+ \to \pi^+ \ell^+ \ell^-$ decays [4].

The amplitude for the $K \to \pi \gamma^*$ decay can be expressed in terms of a single electromagnetic form factor $V(z)$ defined via [2,5]

$$\mathcal{A}_\mu = -i \frac{G_F}{(4\pi)^2} V(z)[q^2(k+p)_\mu - (M_K^2 - M_\pi^2)q_\mu], \quad (1)$$

where μ is the photon polarization index, $z = q^2/M_K^2$, $q = k - p$, and k and p indicate the momenta of the K and π respectively. From analyticity, a prediction of $V(z)$ is given by [2]

$$V(z) = a_+ + b_+ z + V^{\pi\pi}(z), \quad (2)$$

where a_+ and b_+ are free real parameters and $V^{\pi\pi}(z)$ describes the contribution from a $\pi\pi$ intermediate state (detailed in [2]) with a $\pi^+\pi^- \to \gamma^*$ transition. The free parameters have, until recently, only been obtained by fitting experimental data. Having previously measured the K^+ decay channel for electrons and muons at the NA48 experiment at the CERN SPS [6], the follow-up NA62 experiment measured the $K^+ \to \pi^+ \mu^+ \mu^-$ decay during the 2016–2018 run 1 [7], with prospects for further measurements during the 2021–2024 run 2 [8]. From the NA48 electron data, values of $a_+ = -0.578(16)$ and $b_+ = -0.779(66)$ have been found [6], and the available NA62 muon data resulted in $a_+ = -0.592(15)$ and $b_+ = -0.699(58)$ [7].

In parallel, the theoretical understanding of these processes is being improved. The authors of [9,10] construct a theoretical prediction of a_+ and b_+ by considering a two-loop low-energy expansion of $V(z)$

*antonin.portelli@ed.ac.uk

in three-flavor QCD, with a phenomenological determination of quantities unknown at vanishing momentum transfer. From the electron and muon they find $a_+ = -1.59(8)$ and $b_+ = -0.82(6)$, in significant tension with the experimental data fit. The authors acknowledge that more work is being done to estimate more accurately the $\pi\pi$ and KK contributions.

The nonperturbative *ab initio* approach of lattice QCD is well suited to study the dominant long-distance contribution to the matrix element of the $K^+ \to \pi^+ \gamma^*$ decay. Methods with which such a lattice calculation could be performed were first proposed in [11], and additional details on full control of ultraviolet divergences were introduced in [12]. An exploratory lattice calculation [13], using unphysical meson masses, demonstrated a practical application of these methods.

This paper describes a lattice calculation following the same approach as [13], but using physical light-quark masses, thereby allowing for the first time a direct comparison to experiment.

II. EXTRACTION OF THE DECAY AMPLITUDE

The procedure and expressions in this section are largely a summary of the approach described in [13]. We wish to compute the long-distance amplitude defined as

$$\mathcal{A}_\mu(q^2) = \int d^4x \langle \pi(\mathbf{p})|T[J_\mu(0)H_W(x)]|K(\mathbf{k})\rangle \quad (3)$$

in Minkowski space, where q, k, and p are defined as above, J_μ is the quark electromagnetic current and H_W is a $\Delta S = 1$ effective Hamiltonian density, given by [14]

$$H_W = \frac{G_F}{\sqrt{2}} V_{us}^* V_{ud} \sum_{j=1}^{2} C_j(Q_j^u - Q_j^c), \quad (4)$$

where the C_j are Wilson coefficients, and Q_1^q and Q_2^q are the current-current operators defined (up to a Fierz transformation) by [11]

$$Q_1^q = [\bar{s}\gamma_\mu(1-\gamma_5)d][\bar{q}\gamma^\mu(1-\gamma_5)q], \quad (5)$$

$$Q_2^q = [\bar{s}\gamma_\mu(1-\gamma_5)q][\bar{q}\gamma^\mu(1-\gamma_5)d]. \quad (6)$$

We renormalize the operators Q_i^q nonperturbatively within the RI-SMOM scheme [15] and then follow [16] to match to the $\overline{\text{MS}}$ scheme, in which the Wilson coefficients have also been computed.

A. Correlators and contractions

The corresponding Euclidean amplitude—which is accessible to lattice QCD calculations—can be computed with the "unintegrated" 4pt correlator [12]

$$\Gamma_\mu^{(4)}(t_H, t_J, \mathbf{k}, \mathbf{p}) = \int d^3\mathbf{x} \int d^3\mathbf{y} e^{-i\mathbf{q}\cdot\mathbf{x}} \langle \phi_\pi(t_\pi, \mathbf{p})T[J_\mu(t_J, \mathbf{x})$$
$$\times O_W(t_H, \mathbf{y})]\phi_K^\dagger(t_K, \mathbf{k})\rangle, \quad (7)$$

where $\phi_P^\dagger(t, \mathbf{k})$ is the creation operator for a pseudoscalar meson P at time t with momentum $\mathbf{k}$. To obtain the decay amplitude we take the integrated 4pt correlator [12]

$$I_\mu(T_a, T_b, \mathbf{k}, \mathbf{p}) = e^{-(E_\pi(\mathbf{p})-E_K(\mathbf{k}))t_J}$$
$$\times \int_{t_J-T_a}^{t_J+T_b} dt_H \tilde{\Gamma}_\mu^{(4)}(t_H, t_J, \mathbf{k}, \mathbf{p}), \quad (8)$$

in the limit $T_a, T_b \to \infty$. The exponential factor translates the decay to $t_J = 0$, allowing us to omit any t_J dependence in further expressions. Here $\tilde{\Gamma}_\mu^{(4)}$ is the "reduced" correlator, where we have divided out factors that are not included in the final amplitude, i.e.,

$$\tilde{\Gamma}_\mu^{(4)} = \frac{\Gamma_\mu^{(4)}}{Z_{\pi K}}, \qquad Z_{\pi K} = \frac{Z_\pi Z_K^\dagger L^3}{4E_\pi(\mathbf{p})E_K(\mathbf{k})} e^{-t_\pi E_\pi(\mathbf{p})+t_K E_K(\mathbf{k})}, \quad (9)$$

where L^3 is the spatial volume, $Z_\pi = \langle 0|\phi_\pi(\mathbf{p})|\pi(\mathbf{p})\rangle$, $Z_K^\dagger = \langle K(\mathbf{k})|\phi_K^\dagger(\mathbf{k})|0\rangle$, and $E_K(\mathbf{k})$ and $E_\pi(\mathbf{p})$ are the initial-state kaon and final-state pion energies, respectively.

The spectral decomposition of Eq. (7) has been discussed in detail in [13], in particular describing the presence of intermediate one-, two-, and three-pion states between the J_μ and O_W operators. As these states can have energies $E < E_K(\mathbf{k})$ they introduce exponentially growing contributions that cause the integral to diverge with increasing T_a. These contributions do not contribute to the Minkowski decay width [12] and must be removed in order to extract the amplitude

$$A_\mu(q^2) = \lim_{T_a, T_b \to \infty} \tilde{I}_\mu(T_a, T_b, \mathbf{k}, \mathbf{p}), \quad (10)$$

where $\tilde{I}_\mu$ is the integrated 4pt correlator with intermediate-state contributions subtracted. The methods used to remove the intermediate states follow the same steps as in [13], and are outlined in Sec. II B.

The four classes of diagrams—Connected (C), Wing (W), Saucer (S), and Eye (E)—that contribute to the integrated correlator are represented schematically in the Supplemental Material [17]. The current can be inserted on all four quark propagators in each class of diagram, in addition to a quark-disconnected self-contraction. Diagrams of these five current insertions for the C class are also shown in the Supplemental Material [17]. The 20 resulting diagrams need to be computed in order to evaluate Eq. (7).

When working on the lattice there are potentially quadratically divergent contributions that come about as the operators J_μ and H_W approach each other when the current is inserted on the loop of the S and E diagrams [11,12]. Since we perform our calculation with conserved

electromagnetic currents the degree of divergence is reduced to, at most, a logarithmic divergence [11] as a consequence of U(1) gauge invariance and the resulting Ward-Takahashi identity. We emphasize that, due to exact gauge symmetry in lattice QCD there is a vector current, which is exactly conserved on each configuration, independent of any residual chiral symmetry breaking. The remaining logarithmic divergence is removed through the Glashow-Iliopoulos-Maiani (GIM) mechanism [18], implemented here through the inclusion of a valence charm quark in the lattice calculation.

B. Intermediate states

The contribution of the single-pion intermediate state can be removed by either of the two methods discussed in [13]. The first of these (method 1) reconstructs the single-pion state using 2pt and 3pt correlators to subtract its contribution explicitly. The relevant amplitude can be extracted with this method in several ways, including a direct fit of A_μ and the intermediate state, the reconstruction of the intermediate states using fits to 2pt and 3pt correlators, a zero-momentum-transfer approximation and an SU(3)-symmetric-limit approximation, all of which are discussed in detail in [13].

The second method proposed in [13] (method 2) involves an additive shift to the weak Hamiltonian by the scalar density $\bar{s}d$ [19]:

$$O'_W = O_W - c_s \bar{s}d, \qquad (11)$$

where the constant parameter c_s is chosen such that

$$\langle \pi(\mathbf{k})|O'_W|K(\mathbf{k})\rangle = 0. \qquad (12)$$

Replacing O_W with O'_W in Eq. (7) removes the contribution of the single-pion intermediate state. As the scalar density can be written in terms of the divergence of a current, the physical amplitude is invariant under such translation [12]. The two-pion contributions are expected to be insignificant until calculations reach percent-level precision and the three-pion states are even more suppressed [12]. As we do not compute the rare kaon decay amplitude to such a precision, the two- and three-pion states are not accounted for in our studies.

III. DETAILS OF CALCULATION

This calculation is performed on a lattice ensemble generated with the Iwasaki gauge action and $2 + 1$ flavors of Möbius domain wall fermions (DWF) [20]. The spacetime volume is $(L/a)^3 \times (T/a) = 48^3 \times 96$ and the inverse lattice spacing $a^{-1} = 1.730(4)$ GeV. The fifth-dimensional extent is $L_s = 24$ and the residual mass is $am_{\rm res} = 6.102(40) \times 10^{-4}$. The light and strange sea quark masses are $am_l = 0.00078$ and $am_s = 0.0362$ respectively, corresponding to pion and kaon masses of $M_\pi = 139.2(4)$ MeV and $M_K = 499(1)$ MeV. We use 87

gauge configurations, each separated by 20 Monte Carlo time steps.

The Möbius DWF action [21] was used to simulate the sea quarks, with a rational approximation used for the strange quark. In this calculation the light valence quarks make use of the Möbius action [22], an approximation of the Möbius action where the sign function has had its L_s dimension reduced by using complex parameters matched to the original real parameters using the Remez algorithm. This gives a reduced fifth-dimensional extent $L_s = 10$, reducing the computational cost of light-quark inversions. The lowest 2000 eigenvectors of the Dirac operator were also calculated ("deflation"), allowing us to accelerate the light-quark zMöbius inversions further. We correct for the bias introduced by the zMöbius action with a technique similar to all-mode-averaging (AMA) [23] by computing light and charm propagators also using the Möbius action on lower statistics, using the Möbius accelerated DWF algorithm [24] with deflated zMöbius guesses in the inner loop of the algorithm for the light and a mixed-precision solver for the charm quarks. Further details are in the Supplemental Material [17].

The GIM subtraction relies on a precise cancellation, in particular in the low modes of the light and charm actions, and it is paramount to use the same actions for those quarks. With the choice of zMöbius parameters for the light quark, the DWF theory breaks down for the physical charm-quark mass [25]. We instead perform the GIM subtractions using three unphysical charm-quark masses, chosen to be $am_{c_1} = 0.25$, $am_{c_2} = 0.30$, $am_{c_3} = 0.35$, and extrapolate the results to the physical point. The physical charm-quark mass was found to be $am_c = 0.510(1)$ by computing the three unphysical η_c-meson masses and extrapolating to the physical η_c mass. Previous work has demonstrated that, for the lattice parameters in use for this calculation, such an extrapolation is well controlled [26].

We use Coulomb-gauge fixed wall sources for the kaon and pion. The pion and kaon sources are separated by 32 lattice units in time, with the kaon at rest at $t_K = 0$ and the pion with momentum $\mathbf{p} = \frac{2\pi}{L}(1, 0, 0)$ at $t_\pi = 32$. The electromagnetic current is inserted midway between the kaon and the pion at $t_J = 16$, so that the effects of the excited states from the interpolating operators are suppressed. We omit the disconnected diagram, since it is suppressed by SU(3) flavor symmetry and $1/N_c$ to an expected $\sim 10\%$ of the connected-diagram contribution [13]. Given the error on our final result, the disconnected contribution is negligible. Control of the error is being explored in an ongoing project.

We use the Möbius conserved lattice vector current [20] with only the time component $\mu = 0$, which is sufficient to extract the single form factor from Eq. (1).

To compute the loops in the S and E diagrams we use spin-color diluted sparse sources, similar to those used
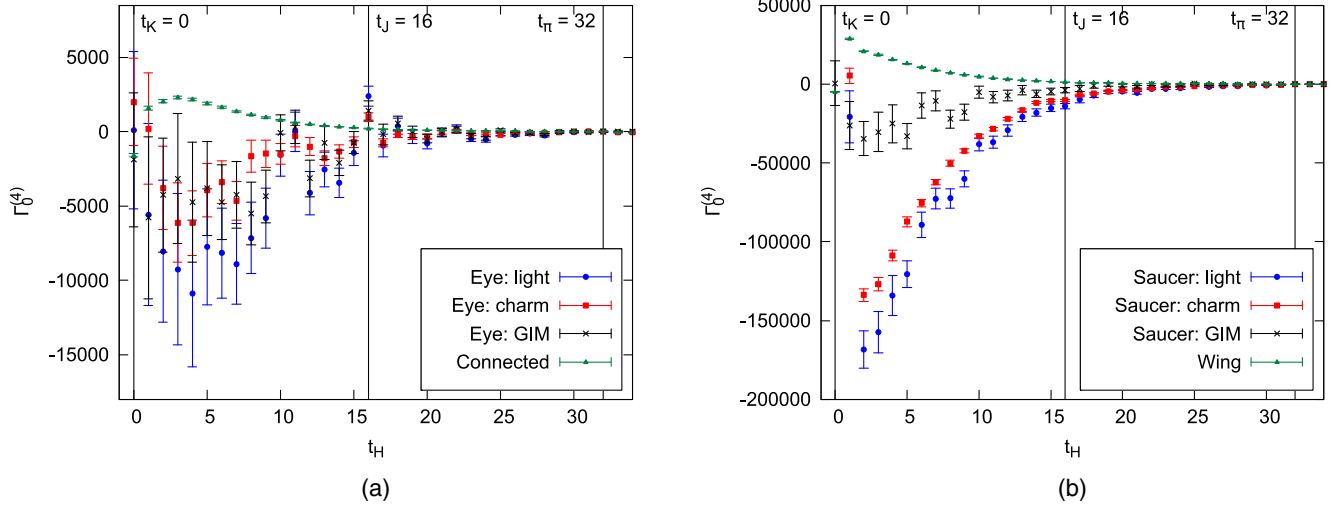
FIG. 1.   The (a) Q_1 and (b) Q_2 operator contributions to the $am_{c_1} = 0.25$ integrated 4pt rare kaon correlator, separated into C, W, S, and E diagrams. The light- and charm-quark contributions to the S and E diagrams are shown individually, as well as their difference, the "GIM" contribution.

in [27], the structure of which is described in the Supplemental Material [17]. We use the AMA technique [23] for our calculation of these diagrams, computing one hit of sparse noise with "exact" solver precision (10^{-8}, 10^{-10}, 10^{-12}, and 10^{-14} for the light, c_1, c_2, and c_3 quarks, respectively) and the same hit of sparse noise with "inexact" solver precision (10^{-4} for all quarks). We then compute an additional nine hits of sparse noise with inexact solver precision and apply a correction computed from the difference of the reciprocal noises.

We performed all correlation function calculations using dedicated software [28] based on the Grid [29,30] and Hadrons [31] libraries. All three are free software under GPLv2. The raw lattice correlators used in this work are publicly available online [32].
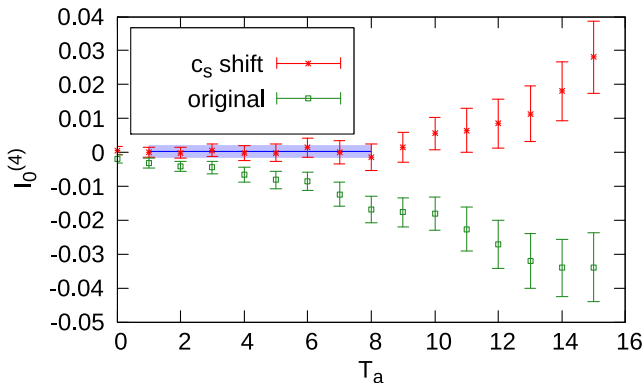

FIG. 2.   The $am_{c_1} = 0.25$ integrated 4pt rare kaon correlator shown for $I_0(T_a, T_b = 8, \mathbf{k}, \mathbf{p})$ [cf. Eq. (8)] to demonstrate the T_a dependence. The green data shows the raw 4pt function, and in red we show the same data after removing the single-pion exponential growth via method 2. The fit to the plateau, shown in blue, gives $A_0 = 0.00022(172)$.

IV. NUMERICAL RESULTS

The 4pt functions for the lightest charm-quark mass are shown in Fig. 1, and Fig. 2 shows the T_a dependence of the integrated correlator for fixed T_b both before and after removing the exponentially growing contributions using method 2. We perform a simultaneous fit to the 2pt, 3pt and integrated 4pt functions, extracting matrix elements, energies, form factors and A_0, using a covariance matrix with fully correlated 2pt and 3pt sectors and uncorrelated 4pt sector. From this fit, we obtain $A_0 = 0.00022(172)$ with a $\chi^2/\mathrm{dof} = 0.996$. Further details on the fitting procedure, including a discussion of the fit ranges which were used, are presented in the Supplemental Material [17]. The error on A_0 is entirely statistical.

Table I shows the results for A_0 using the three charm-quark masses, extracted using the different methods detailed above. The results from method 2 have statistical

TABLE I.   Fit results for A_0 for the three unphysical charm-quark masses and value found from extrapolating these to the physical point. The first four results are obtained using the various approaches to method 1, as described in Sec. II B, and the final result is obtained using method 2.

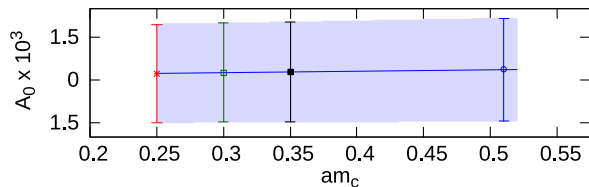| Analysis	m_{c_1}	m_{c_2}	m_{c_3}
Method 1			
Direct fit	$-0.00052(208)$	$-0.00046(210)$	$-0.00040(211)$
2pt/3pt recon	$-0.00036(162)$	$-0.00024(164)$	$-0.00017(165)$
0 mom transfer	$-0.00087(165)$	$-0.00086(166)$	$-0.00086(167)$
$SU(3)$ symm lim	$0.00055(165)$	$0.00085(166)$	$0.00112(167)$
Method 2			
c_s shift	$0.00022(172)$	$0.00024(173)$	$0.00027(174)$

FIG. 3. The extrapolation of the A_0 results found using method 2 to the physical charm-quark mass. The linear fit and extrapolated result are shown in blue, giving a result of $A_0 = 0.00035(180)$. Red, green, and black show the results at the c masses we simulate at, and we extrapolate those to the blue data point at physical charm mass.

errors compatible with method 1 results. As method 2 has the simplest fit structure, we use it to extrapolate to the physical charm-quark mass and to compute the form factor as our final result. We stress that method 1 remains an important cross-check on the analysis. Figure 3 shows the extrapolation of the method 2 results to the physical charm-quark mass, giving a value of $A_0 = 0.00035(180)$. From Eq. (1) we can relate our result to the form factor to achieve $V(z) = -0.87(4.44)$. For our choice of kinematics we have $z = 0.013(2)$; we expect the b_+z contribution to be $\sim 10^{-2}$ assuming b_+ is $\mathcal{O}(1)$, and we estimate $V^{\pi\pi}(z) = -0.00076(73)$ following [2]. We may therefore take our result for a_+ as an approximation for the intercept of the form factor.

V. CONCLUSION

We have carried out the first lattice QCD calculation of the $K^+ \to \pi^+ \ell^+ \ell^-$ decay amplitude using physical pion and kaon masses. When using physical light-quark masses, even with unphysically light charm-quark masses, the contributions in the GIM loops statistically decorrelate, as shown in Fig. 4. This contributes to the unsatisfactory

amount of noise in GIM subtraction, as can be seen in Fig. 1. Although sparse noises reduced the statistical error introduced by the single-propagator trace contribution to the Eye and Saucer diagrams, we are not able to obtain a well-resolved result for the amplitude.

The form factor that encapsulates the behavior of the long-distance amplitude of the rare kaon decay was found to be $V(0.013(2)) = -0.87(4.44)$. When this is compared to experimental results, $V^{\exp}(0) \equiv a_+^{\exp} = -0.578(16)$ from the electron and $a_+^{\exp} = -0.592(15)$ from the muon, it can be seen that the error on our lattice result is about 8 times larger than the central value of the experimental result. However, our error is 3 times larger than the phenomenological central value obtained in [9,10], which suggests that lattice QCD calculations will be able to provide a competitive theoretical bound on a_+ in the coming years.

We would like to stress that since the noise emerges mainly from the lack of correlation in the GIM subtraction, the error obtained here has the potential to be reduced beyond square-root scaling by optimizing the stochastic estimator used for the up-charm loops. Such problems have common elements with similar challenges in computing quark-disconnected diagrams, for example as discussed in [33].

Finally, it might also be possible to work in three-flavor QCD, forgoing the calculation of the charm-quark loop [34], further reducing computational costs. This would require a new renormalization procedure which would be analogous to that of the $K \to \pi\nu\bar{\nu}$ study that was performed by the RBC-UKQCD collaborations previously [35,36].

In conclusion, despite obtaining a first physical result with a large uncertainty, we believe that optimization of the methodology, combined with the increased capabilities of future computers, should allow for a competitive prediction of the $K^+ \to \pi^+ \ell^+ \ell^-$ amplitude within the next years.
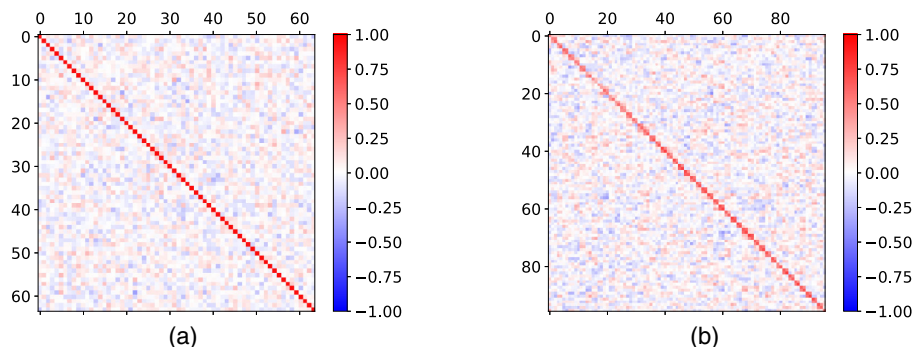

FIG. 4. The cross-correlation in the Eye diagram between the light-quark and the lightest charm-quark correlation functions for (a) the exploratory study [13] at heavier-than-physical light-quark mass and (b) the calculation reported on in this work at physical light-quark mass. Although equal time slices exhibit a distinguishable correlation in both cases, it is greatly diminished in the physical-point calculation. This results in a poor statistical cancellation in the GIM loop, driving the large statistical error from this calculation.

ACKNOWLEDGMENTS

[1] P. Zyla *et al.* (Particle Data Group), Review of particle physics, Prog. Theor. Exp. Phys. **2020**, 083C01 (2020).

[2] G. D'Ambrosio, G. Ecker, G. Isidori, and J. Portolés, The decays $K \to \pi \ell^+ \ell^-$ beyond leading order in the chiral expansion, J. High Energy Phys. 08 (1998) 004.

[3] R. Aaij *et al.* (LHCb Collaboration), Test of lepton universality in beauty-quark decays, Nat. Phys. **18**, 277 (2022).

[4] A. Crivellin, G. D'Ambrosio, M. Hoferichter, and L. C. Tunstall, Violation of lepton flavor and lepton flavor universality in rare kaon decays, Phys. Rev. D **93**, 074038 (2016).

[5] V. Cirigliano, G. Ecker, H. Neufeld, A. Pich, and J. Portolés, Kaon decays in the standard model, Rev. Mod. Phys. **84**, 399 (2012).

[6] J. Batley *et al.*, Precise measurement of the $K^+ \to \pi^+ e^+ e^-$ decay, Phys. Lett. B **677**, 246 (2009).

[7] L. Bician *et al.*, New measurement of the $K^+ \to \pi^+ \mu^+ \mu^-$ decay at NA62, Proc. Sci. ICHEP2020 (**2021**) 364.

[8] C. Lazzeroni (NA62 Collaboration), 2021 NA62 status report to the CERN SPSC, Status Reports No. CERN-SPSC-2021-009 and No. SPSC-SR-286, CERN SPS, 2021, https://cds.cern.ch/record/2759557.

[9] G. D'Ambrosio, D. Greynat, and M. Knecht, On the amplitudes for the *CP*-conserving $K^\pm(K_S) \to \pi^\pm(\pi^0)\ell^+\ell^-$ rare decay modes, J. High Energy Phys. 02 (2019) 049.

[10] G. D'Ambrosio, D. Greynat, and M. Knecht, Matching long and short distances in the form factors for $K \to \pi\ell^+\ell^-$, Phys. Lett. B **797**, 134891 (2019).

[11] G. Isidori, G. Martinelli, and P. Turchetti, Rare kaon decays on the lattice, Phys. Lett. B **633**, 75 (2006).

[12] N. H. Christ, X. Feng, A. Portelli, and C. T. Sachrajda, Prospects for a lattice computation of rare kaon decay amplitudes: $K \to \pi\ell^+\ell^-$ decays, Phys. Rev. D **92**, 094512 (2015).

[13] N. H. Christ, X. Feng, A. Jüttner, A. Lawson, A. Portelli, and C. T. Sachrajda (RBC and UKQCD Collaborations), First exploratory calculation of the long-distance contributions to the rare kaon decays $K \to \pi\ell^+\ell^-$, Phys. Rev. D **94**, 114516 (2016).

[14] G. Buchalla, A. J. Buras, and M. E. Lautenbacher, Weak decays beyond leading logarithms, Rev. Mod. Phys. **68**, 1125 (1996).

[15] C. Sturm, Y. Aoki, N. H. Christ, T. Izubuchi, C. T. C. Sachrajda, and A. Soni, Renormalization of quark bilinear operators in a momentum-subtraction scheme with a non-exceptional subtraction point, Phys. Rev. D **80**, 014501 (2009).

[16] C. Lehner and C. Sturm, Matching factors for $\Delta S = 1$ four-quark operators in RI/SMOM schemes, Phys. Rev. D **84**, 014001 (2011).

[17] See Supplemental Material at http://link.aps.org/supplemental/10.1103/PhysRevD.107.L011503 for further details on the sparse sources, correlation functions and fit procedures employed in this work.

[18] S. L. Glashow, J. Iliopoulos, and L. Maiani, Weak interactions with lepton-hadron symmetry, Phys. Rev. D **2**, 1285 (1970).

[19] Z. Bai, N. H. Christ, T. Izubuchi, C. T. Sachrajda, A. Soni, and J. Yu, $K_L - K_S$ Mass Difference from Lattice QCD, Phys. Rev. Lett. **113**, 112003 (2014).

[20] T. Blum *et al.* (RBC and UKQCD Collaborations), Domain wall QCD with physical quark masses, Phys. Rev. D **93**, 074505 (2016).

[21] R. Brower, H. Neff, and K. Orginos, The Möbius domain wall fermion algorithm, Comput. Phys. Commun. **220**, 1 (2017).

[22] G. McGlynn, Algorithmic improvements for weak coupling simulations of domain wall fermions, Proc. Sci. LATTICE2015 (**2016**) 019.

[23] T. Blum, T. Izubuchi, and E. Shintani, New class of variance-reduction techniques using lattice symmetries, Phys. Rev. D **88**, 094503 (2013).

[24] H. Yin and R. D. Mawhinney, Improving DWF simulations: The force gradient integrator and the Möbius accelerated DWF solver, Proc. Sci., LATTICE2011 (**2011**) 051.

[25] P. Boyle, A. Jüttner, M. K. Marinković, F. Sanfilippo, M. Spraggs, and J. T. Tsang, An exploratory study of heavy domain wall fermions on the lattice, J. High Energy Phys. 04 (2016) 124.

[26] P. A. Boyle, L. Del Debbio, A. Jüttner, A. Khamseh, F. Sanfilippo, and J. T. Tsang, The decay constants f_D and f_{D_s} in the continuum limit of nf $= 2 + 1$ domain wall lattice QCD, J. High Energy Phys. 12 (2017) 008.

[27] T. Blum, P. A. Boyle, T. Izubuchi, L. Jin, A. Jüttner, C. Lehner, K. Maltman, M. Marinkovic, A. Portelli, and M. Spraggs (RBC and UKQCD Collaborations), Calculation of the Hadronic Vacuum Polarization Disconnected Contribution to the Muon Anomalous Magnetic Moment, Phys. Rev. Lett. **116,** 232002 (2016).

[28] F. Ó hÓgáin, F. Erben, and A. Portelli, Simulating rare kaon decays using domain wall lattice QCD with physical light quark masses, 10.5281/zenodo.6369186.

[29] P. A. Boyle, G. Cossu, A. Yamaguchi, and A. Portelli, Grid: A next generation data parallel C++ QCD library, Proc. Sci., LATTICE2015 (**2016**) 023.

[30] P. Boyle, G. Cossu, G. Filaci, C. Lehner, A. Portelli, and A. Yamaguchi, Grid: OneCode and FourAPIs, Proc. Sci., LATTICE2021 (**2022**) 035 [arXiv:2203.06777].

[31] A. Portelli, R. Abott, N. Asmussen, A. Barone, P. A. Boyle, F. Erben, N. Lachini, M. Marshall, V. Gülpers, R. C. Hill, R. Hodgson, F. Joswig, F. Ó hÓgáin, and J. P. Richings, aportelli/hadrons: Hadrons v1.3 (2022).

[32] P. A. Boyle, F. Erben, J. M. Flynn, V. Gülpers, R. C. Hill, R. Hodgson, A. Juettner, F. Ó hÓgáin, A. Portelli, and C. T. Sachrajda, Simulating rare kaon decays using domain wall lattice QCD with physical light quark masses, 10.5281/zenodo.6369178.

[33] L. Giusti, T. Harris, A. Nada, and S. Schaefer, Frequency-splitting estimators of single-propagator traces, Eur. Phys. J. C **79,** 586 (2019).

[34] A. Lawson, Exploratory lattice QCD studies of rare kaon decays, Ph.D. thesis, University of Southampton, 2017.

[35] N. H. Christ, X. Feng, A. Portelli, and C. T. Sachrajda, Prospects for a lattice computation of rare kaon decay amplitudes. II. $K \to \pi \nu \bar{\nu}$ decays, Phys. Rev. D **93,** 114517 (2016).

[36] Z. Bai, N. H. Christ, X. Feng, A. Lawson, A. Portelli, and C. T. Sachrajda, Exploratory Lattice QCD Study of the Rare Kaon Decay $K \to \pi \nu \bar{\nu}$, Phys. Rev. Lett. **118,** 252001 (2017).

[37] https://www.dirac.ac.uk/.